J. Phys. D: Appl. Phys., Vol. 11, 1978. Printed in Great Britain

Theory of particle capture in axial filters for high gradient magnetic separation

R Gerber
Department of Pure and Applied Physics, University of Salford, Salford M5 4WT

Received 15 February 1978, in final form 15 April 1978

Abstract. A theory of capture of magnetic particles, in axially ordered filters, carried by laminar flow of a viscous fluid is presented. The particle trajectories are obtained in an analytical nearly closed form. This facilitates the numerical computation of isotelic curves and, since these demarcate the capture area, the determination of the filter performance. The particle trajectories, the particle capture length and the filter performance do not depend on the viscosity of the particle carrying fluid. However, they are in general different from those predicted by previous theories of capture in ideal flow. The main difference, as far as the filter performance is concerned, lies in a more complicated relationship between the capture area and the normalised capture length. The fact that the inflow and escape velocities have different magnitudes is less significant.

1. Introduction

High gradient magnetic separation (HGMS) is a method for the removal of micron-sized magnetic particles from suspensions. It has attracted considerable attention in recent years, because the technique, already used commercially in mineral processing, offers the prospect of solving complicated problems encountered in the chemical, nuclear, biochemical, pharmaceutical and other industries. Moreover, the application of this method is not restricted to the production side of the industrial process but it can also be used for effluent treatment and general pollution control (Watson 1977, de Latour and Kolm 1975). Consequently, HGMS may become an important part of future technology and it is therefore desirable to understand its physics in detail. Fundamental to the magnetic separation process is the mechanism of particle capture. A number of papers have already treated this subject (Watson 1973, 1975, Luborsky and Drummond 1975, Birss *et al* 1976, Cowen *et al* 1976, Uchiyama *et al* 1976). The theory described by them has been restricted to the so-called 'inviscid' approximation, in which the fluid is considered to be ideal when interacting with the wires of the filter but viscous when interacting with the particles. The consequence of this inconsistency is that the results of these papers might be expected to give some discrepancies when compared with bulk or average measurements, but when individual particles are investigated disagreements of a fundamental nature are bound to appear.

Models of particle capture assuming the fluid to be viscous in relation to both particles and wires have only recently been described (Cummings *et al* 1976, Clarkson *et al* 1976). They are concerned with a configuration where the magnetic field and the fluid flow are parallel and both are perpendicular to the wire axis. Here it is difficult to obtain an

0022-3727/78/0015-2119 $02.00

analytical expression which simultaneously describes the fluid flow at close range and at large distances from the wire. Consequently, these models are of a predominantly numerical character.

The aim of this paper is to develop a consistent model which will analytically describe, as far as is possible, the particle capture in laminar flow. The calculations are therefore performed for the axial configuration, i.e. the fluid flow is considered to be parallel and the magnetic field perpendicular to the axes of mutually parallel wires of an ordered filter.

2. Single wire

2.1. Trajectories

Consider a ferromagnetic wire of radius a and saturation magnetisation M_s placed coaxially in a tube of nonmagnetic material along the z axis of a cartesian coordinate system (figure 1). The radius of the tube $\bar{r}$ can be expressed in terms of the radius a as $\bar{r}_a=\bar{r}/a$ and this convention of using subscript a to indicate this renormalisation will be used with other quantities throughout. Both the wire and the tube have the same length l_a. A uniform magnetic field H_0, large enough to saturate the wire, is applied in the x direction. Spherical paramagnetic particles of radius R_a ($R_a \ll 1$) and susceptibility χ are carried by a fluid of viscosity η which flows between the wire and the tube in the positive z direction. The flow of the fluid is considered to be laminar, the pressure difference between the beginning and the end of the tube is P_0. The particles are assumed to experience a viscous force given by Stokes' law.

The radial distribution of the fluid velocity v_a is governed by the differential equation (Landau and Lifshitz 1966)

$$\frac{1}{r_a}\frac{\mathrm{d}}{\mathrm{d}r_a}\left(r_a\frac{\mathrm{d}v_a}{\mathrm{d}r_a}\right)=\frac{P_0}{\eta l_a} \tag{1}$$

the solution of which is

$$v_a=\frac{P_0}{4\eta l_a}(1-r_a^2+q\ln r_a) \qquad 1\leqslant r_a\leqslant \bar{r}_a \tag{2}$$

where

$$q=2r_{aq}^2=(\bar{r}_a^2-1)/\ln \bar{r}_a$$

and r_{aq} is the radius where v_a attains its maximum in the interspace between the wire and the tube.

Integration of v_a over the cross-section of the interspace gives the average fluid velocity $\bar{V}_0$ as

$$\bar{V}_0=\frac{P_0 a}{8\eta l_a}\left[\bar{r}_a^2+1-\left(\frac{\bar{r}_a^2-1}{\ln \bar{r}_a}\right)\right]. \tag{3}$$

The particle motion can be conveniently described in terms of cylindrical coordinates r_a, θ and z_a, which are related to the Cartesian ones by the relations

$$x_a=r_a\cos\theta$$

$$y_a=r_a\sin\theta$$

and

$$z_a=z_a.$$

The equations of motion can be derived by a procedure analogous to that of Watson (1973) and used by Birss *et al* (1976) in treating the ideal flow case. The difference is, however, that instead of the ideal flow velocity V_0 and the magnetic velocity V_m the pressure difference P_0 and the magnetic pressure coefficient P_m are introduced by equation (2) and $V_m/a = P_m/4\eta l_a$. If the inertia of the particle is neglected, the equations of motion for the laminar flow case take the form

$$\frac{dr_a}{dt} = -\frac{P_m}{4\eta l_a}\left(\frac{K}{r_a^5} + \frac{\cos 2\theta}{r_a^3}\right) \tag{4}$$

$$r_a \frac{d\theta}{dt} = -\frac{P_m}{4\eta l_a}\frac{\sin 2\theta}{r_a^3} \tag{5}$$

$$\frac{dz_a}{dt} = \frac{P_0}{4\eta l_a}(1 - r_a^2 + q \ln r_a) \qquad 1 \leqslant r_a \leqslant \bar{r}_a \tag{6}$$

where $P_m = \frac{8}{9}\chi H_0 M_s R_a^2 l_a$ is the magnetic pressure coefficient. This coefficient is of magnetic origin and is independent of viscosity. It has dimensions of pressure. The constant $K = M_s/2\mu_0 H_0$ and $\mu_0 = 4\pi \times 10^{-7}$ H m^{-1}. SI units (Kennelly system) are used throughout.

If the time is eliminated from (4), (5) and (6) the set of differential equations

$$\frac{dr_a}{d\theta} = \frac{K}{r_a \sin 2\theta} + r_a \cot 2\theta \tag{7}$$

$$\frac{dz_a}{d\theta} = -\frac{P_0}{P_m}\frac{(1 - r_a^2 + q \ln r_a) r_a^4}{\sin 2\theta} \tag{8}$$

determining the trajectory of the particle is obtained.

One important fact is immediately apparent: η does not enter into (7) and (8) at all. Thus neither the shape of the trajectory nor the capture length depend on the viscosity of the fluid carrying the particles. Consequently, the performance of the filter, at least in the single-wire approximation, is also independent of η. It is the throughput, which is inversely proportional to η.

The equation (7) is the same as the corresponding one in the ideal flow case (Birss *et al* 1976). It can be solved analytically and the solution

$$r_a = (-K \cos 2\theta + C\,|\sin 2\theta|)^{1/2} \tag{9}$$

describes a family of trajectory projections on the xy plane.

Two such curves (dashed curves) are shown, in the first quadrant, in figure 1; the curves in the other quadrants can be obtained by symmetry operations with respect to the x and y axes. The constant C is determined by the initial conditions, that is by the position $\{r_{ai}, \theta_i\}$ of the particle when entering the tube. The magnetisation M_s is considered to be saturated and consequently, if H_i is the internal field in the wire, it holds $H_i \geqslant 0$. As the demagnetising factor, in the direction perpendicular to the wire axis, is $\frac{1}{2}$, the constant K satisfies the relation $0 \leqslant K \leqslant 1$. As $r_{ai} \geqslant 1$ always holds, the constant C satisfies $C \geqslant (1 - K^2)^{1/2}$. A trajectory projection starts on the unit circle at an angle θ_s (near to the y axis), follows a path reaching a maximum excursion r_{amax} and returns to the unit circle at an angle θ_e (near to the x axis). The angles θ_s and θ_e are given by

$$\theta_{s,e} = \frac{1}{2}\arccos\left(\frac{-K \mp |C|\,(K^2 + C^2 - 1)^{1/2}}{K^2 + C^2}\right) \tag{10}$$

where the minus and plus sign corresponds to θ_s and θ_e, respectively.

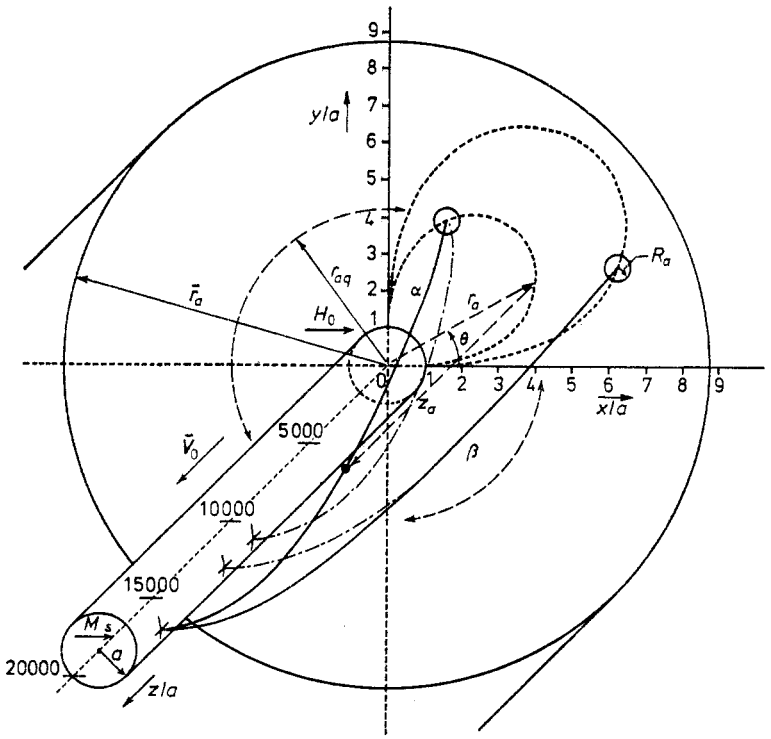

Figure 1. Trajectories in laminar and ideal flow. Laminar flow trajectories, ————; ideal flow trajectories, —— - - ——; trajectory projections, - - -. Parameters: $K=0{\cdot}8$, $r_{a\max}=5$ and 8, $q=35$, $\bar{r}_a=8{\cdot}7752$, $r_{aq}=4{\cdot}1833$, $P_0/P_m=1$, $V_0/V_m=21{\cdot}51074$, $F\approx 0{\cdot}07$.

The quantity $r_{a\max}=(K^2+C^2)^{1/4}$ can be used to label the trajectory projections. Two of those shown in figure 1 were calculated for typical values of $K=0{\cdot}8$, $r_{a\max}=5$ and 8.

The equation (8), describing the progress of the particle along the z axis, is different from and more complicated than the corresponding one in the ideal flow case. Nevertheless it can be solved analytically in a nearly closed form. The solution of (8), depending on the initial position $\{r_{ai}, \theta_i\}$ and the current position $\{r_a, \theta\}$, can be obtained as

$$z_a=\frac{P_0}{P_m}[I_1(\theta)+I_2(\theta)+qI_3(\theta)]_0^{\theta_i}. \tag{11}$$

The functions $I_1(\theta)$, $I_2(\theta)$ and $I_3(\theta)$ are

$$I_1(\theta)=\frac{K^2}{2}\ln|\tan\theta|-Kr_a{}^2-\frac{K^2+C^2}{2}\cos 2\theta \tag{11a}$$

$$I_2(\theta)=\frac{r_a{}^2}{2}\left(Kr_a{}^2+\frac{K^2+C^2}{2}\cos 2\theta\right)+\frac{K^3}{2}\ln|\sin 2\theta|-\frac{C(C^2+3K^2)}{2}\frac{|\sin 2\theta|}{\sin 2\theta}\,\theta, \tag{11b}$$

$$I_3(\theta)=\frac{K^2+C^2}{4}\left(\frac{C}{(K^2+C^2)^{1/2}}\ln\left|\frac{K|\tan\theta|+C-(K^2+C^2)^{1/2}}{K|\tan\theta|+C+(K^2+C^2)^{1/2}}\right|+\cos 2\theta\right)$$
$$+\frac{K}{2}r_a{}^2-\left(Kr_a{}^2+\frac{K^2+C^2}{2}\cos 2\theta\right)\ln r_a+K^2\sum_{l=1}^{p}\frac{\ln r_a(\theta_l)}{p\sin 2\theta_l}(\theta-\theta_s) \tag{11c}$$

where $\theta_l=\theta_s+(2l-1)(\theta-\theta_s)/2p$.

The primitive function of one of the integrals in $I_3(\theta)$ most probably cannot be expressed in closed form. It was therefore approximated by a finite series. This approximation works very well as far as the trajectory as a whole is concerned. The solution (11) was checked, with increasing p, against the computed 'exact' solution, represented by an accurate, though more time-consuming, numerical integration of (8). The maximum error, for a value of p as low as 3, $K=0{\cdot}8$, in any individual point of any trajectory with $r_{a\max} \geqslant 2$ is found to be less than 1 %. The error decreases with increasing p and $r_{a\max}$.

This and all other computations in this paper were carried out on the ICL 1904S computer at the University of Salford using both the author's and NAG standard procedures (NAG Ltd, 7 Banbury Road, Oxford OX2 6NN).

If $\theta_1=0$, then also $\theta=0$. The time can be eliminated from (4) and (6) giving the differential equation

$$\frac{\mathrm{d}z_a}{\mathrm{d}r_a} = -\frac{P_0}{P_\mathrm{m}} \frac{(1-r_a{}^2+q \ln r_a) r_a{}^5}{K+r_a{}^2} \tag{12}$$

for the trajectory in the xz plane. The solution of (12) can be obtained as

$$z_a = \frac{P_0}{P_\mathrm{m}} [J_1(r_a)+qJ_2(r_a)]_{r_a}^{r_{a1}}. \tag{13}$$

The functions $J_1(r_a)$ and $J_2(r_a)$ are

$$J_1(r_a) = -\frac{r_a{}^6}{6}+(K+1)\frac{r_a{}^4}{4}-K(K+1)\frac{r_a{}^2}{2}+\frac{K^2(K+1)}{2}\ln|K+r_a{}^2| \tag{13a}$$

$$J_2(r_a) = \left(\frac{r_a{}^4}{8}-K\frac{r_a{}^2}{4}+\frac{K^2}{4}\ln|K+r_a{}^2|\right)\ln r_a{}^2-\frac{r_a{}^4}{16}$$

$$+K\frac{r_a{}^2}{4}-\frac{K^2}{8}\ln^2 r_a{}^2-K^2\sum_{n=1}^{p}\frac{(-1)^n}{(2n)^2}\left(\frac{K}{r_a{}^2}\right)^n. \tag{13b}$$

An approximation, analogous to that used in (11*c*), had to be introduced in (13*b*). Its effect on the solution (13) is of a similar nature to that mentioned above, when discussing the solution (11).

Two trajectories, given by solutions (9) and (11), for two different initial positions are shown by the solid curves in figure 1. Their characteristic parameters are $K=0{\cdot}8$, $r_{a\max}=5$ and 8, $P_0/P_\mathrm{m}=1$ and $q=35$. These trajectories for laminar flow conditions can be compared with the trajectories (dot-and-dash curves in figure 1) starting at the same initial positions but calculated for the assumption of ideal flow. The calculation was performed using formulae (9) and

$$z_a=(V_0/V_\mathrm{m})[I_1(\theta)]_{\theta_i}^{\theta_1},$$

which describe trajectories for the ideal flow case. The ratio V_0/V_m can be obtained by identifying V_0 with the average velocity $\bar{V}_0$, given by (3), and using the fact that $V_\mathrm{m}=P_\mathrm{m}a/4\eta l_a$. The value of V_0/V_m, for the ideal flow trajectories in figure 1, was found to be 21·51074.

It can be seen that the two types of trajectories differ in their shape and capture length. Consequently, the capture area associated with a single wire is different for the laminar and ideal flow case.

The analytical solutions (11) and (13) are significant for two reasons. Firstly, they make it easy to compare theory with experiment in general without being limited to a

certain range of parameters, as is the case with numerically computed solutions. Secondly, they are the necessary prerequisite for the numerical computation of isotelic curves and, as these curves demarcate the capture area, for finding the performance of the filter.

2.2. Isotelic curves

It is convenient to define the normalised capture length L_a as

$$L_a = \frac{P_m z_{ae}}{P_0} \tag{14}$$

where z_{ae} is the actual wire length necessary to capture the particle. The quantity z_{ae} can be calculated from (11) and (9) (or from (13) if $\theta_i = 0$) by substituting the initial position $\{r_{ai}, \theta_i\}$ and the end position $\{r_a = 1, \theta = \theta_e\}$.

The isotelic curve is then defined as the locus of points $\{r_{ai}, \theta_i\}$ for which L_a has a constant value.

'Isotelic' indicates that the capture occurs at the same distance from the origin. This term is a counterpart to isochronal which indicates that the capture occurs after the same period of time and which is applicable to the ideal case. For example, both particles in figure 1 are on an isotelic curve for the laminar flow conditions.

The isotelic curves can be numerically computed for various L_a and q using (9), (10), (11) and (13). This was performed for a typical value of $K = 0{\cdot}8$ and eighteen values of q from $\langle 10, 2500 \rangle$, where for each q a family of eleven isotelic curves, for various L_a, was obtained. The values of L_a were in the range between zero and an upper limit determined by the substitution of $\bar{r}_a$ into (13). An example of a family of isotelic curves for $K = 0{\cdot}8$, $q = 35$ and various values of L_a is shown in figure 2. The largest isotelic curve in figure 2 is the last one which fits completely inside the tube of radius $\bar{r}_a$. Thus the normalised capture length $L_a = 2{\cdot}447 \times 10^4$ which corresponds to this curve represents the limit of validity of the theory describing the capture on a single wire in a concentric tube for values $K = 0{\cdot}8$ and $q = 35$.

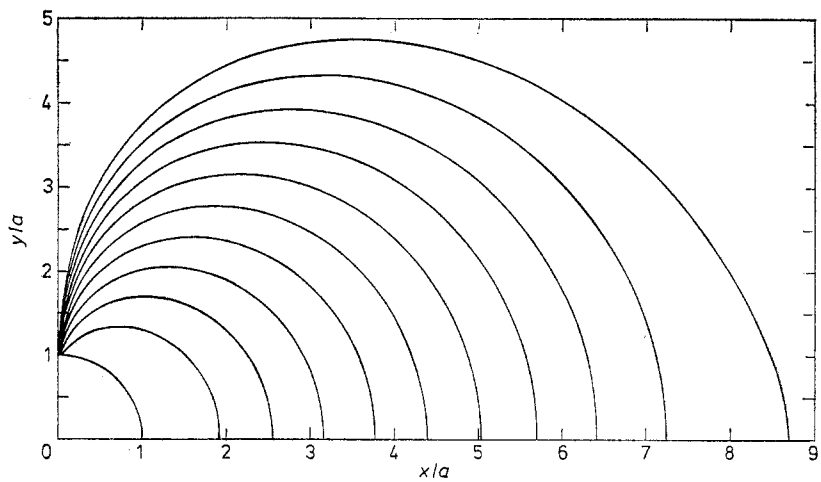

Figure 2. A family of isotelic curves for $K = 0{\cdot}8$, $q = 35$ and $L_a = 0$, $3{\cdot}609 \times 10$, $1{\cdot}863 \times 10^2$, $5{\cdot}699 \times 10^2$, $1{\cdot}346 \times 10^3$, $2{\cdot}702 \times 10^3$, $4{\cdot}837 \times 10^3$, $7{\cdot}948 \times 10^3$, $1{\cdot}220 \times 10^4$, $1{\cdot}770 \times 10^4$, $2{\cdot}447 \times 10^4$. The capture area increases monotonically with increasing L_a.

The capture area A_a is given by the area enclosed by the four isotelic curves at the wire, obtained by symmetrical operations with respect to the x and y axes. The area A_a was evaluated by numerical integration for all isotelic curves computed previously. In this region of investigation, it was found that the area A_a can be expressed, with a maximum error, at any point, of less than 1 %, as

$$A_a = \sum_{i=0}^{6} a_i (L_a)^{i/4} \tag{15}$$

where $a_0 = \pi$ and the other $a_i (a_0, a_1, a_2, a_4$ and $a_6 > 0$, a_3 and $a_5 < 0)$ are functions of q only. Figure 3 shows all the coefficients a_i versus q over the investigated region.

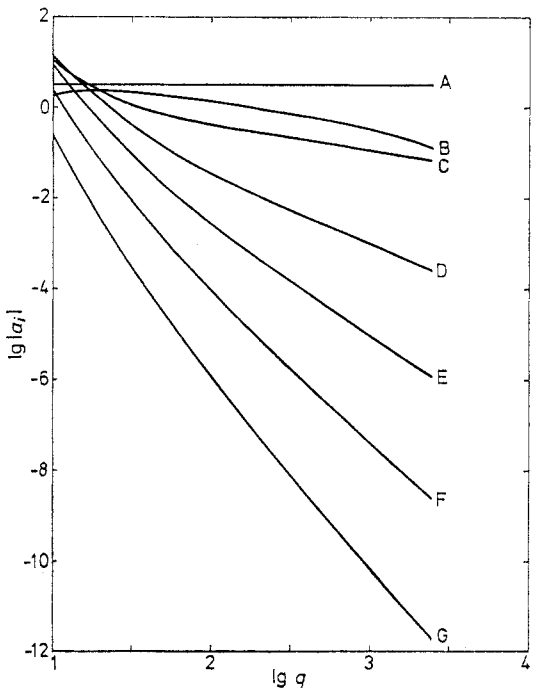

Figure 3. Coefficients a_i $(i=0, 1, 2, \ldots 6)$ for $K=0{\cdot}8$ as a function of q. Curves: A lg a_0, B lg a_1, C lg a_2, D lg $(-a_3)$, E lg a_4, F lg $(-a_5)$, G lg a_6.

The capture area A_a in the ideal flow case is proportional to $(L_a)^{1/2}$ and independent of q. Since the quantity q is related to the boundary of the problem considered here, one can conclude that the more complicated nature of (15) is due to the delimitation of the fluid flow. In the case of a multiwire filter this will mean that the influence of other wires on the capture mechanism of the 'representative' single wire is taken into account.

3. Multiwire filter

3.1. Single-wire approximation

An axial multiwire filter consists of a large number of thin ferromagnetic wires of radius a, which are all aligned essentially parallel to one another and also parallel to the direction of fluid flow. A magnetic field, sufficient to produce saturation magnetisation in the

direction perpendicular to the wire axes, is applied. The distribution of wires in a plane orthogonal to the fluid flow is considered to be random and n, the number of wires per unit area, constant over the filter cross-section. The filling factor F is given by $F=n\pi a^2$. This factor can differ from one filter to another, depending on the construction and purpose. A typical value of F is about 0·07, which means that most of the filter's space is not occupied by wires. This helps to suggest a model for an axial multiwire filter. A statistical average of velocity distributions in an annular space around each wire of the filter can be established. The statistical average has full axial symmetry and can be identified with expression (2). Thus a multiwire filter is replaced by a set of 'representative' single wires of identical environment, the values of a and n being kept unchanged.

It remains to determine the parameter $q=2r_{aq}^2$, $q\geqslant 2$, in the expression (2). This can be done by linking q to ρ_0, the specific fluid impedance of the unloaded filter, defined by

$$P_0=\rho_0(l/S)Q \tag{16}$$

where P_0 is the pressure difference, Q the fluid discharge, l the length and S the cross-section of the multiwire filter, all quantities to be determined experimentally.

The discharge Q can, however, also be given as $Q=nSQ_w$, where

$$Q_w=2\pi a^3\int_1^{r_{aq}} r_a v_a \,\mathrm{d}r_a$$

is the discharge associated with one 'representative' wire. Evaluating Q, in terms of q and F, and substituting in (16) gives, after rearrangement,

$$\frac{8\eta}{a^2F}\frac{1}{\rho_0}=-1+2q+\frac{q^2}{4}\left(\ln\frac{q^2}{4}-3\right). \tag{17}$$

The left-hand side of (17) contains only experimental quantities, the right-hand side is an implicit function in q. Thus q can be found numerically for a given unloaded multiwire filter.

In the absence of experiment, q can be roughly estimated for a given filter by assuming that the wires are arranged in a regular hexagonal pattern in a plane orthogonal to the fluid flow. Then r_{aq} can be approximated by the distance from a wire to the position of maximum fluid velocity, i.e. $r_{aq}\approx(2\pi/3F\sqrt{3})^{1/2}$, and thus $q\approx 4\pi/3F\sqrt{3}$. The value of q is expected, in practice, to be larger than this estimate owing to the random distribution of wires and fluctuations in n.

If the wires of the filter are not rigid enough to stay in their positions when a magnetic field is applied (or alternatively if they are not fixed) the specific impedance ρ_0 will change due to the displacement of the wires from their equilibrium positions (Parker and Sheerer 1977 private communication). In this case the appropriate value of ρ_0 in (17) is the experimental value of the specific impedance measured in the presence of the same magnetic field H_0 which is used to operate the separator.

The concept just outlined links the capture mechanism on a single wire in a concentric tube to that of a multiwire filter. There is, however, a difference in the limit of validity of the theory. In a multiwire filter the theory is valid only up to the radius r_{aq}, since this is the extremity, where the areas of competing influence of adjacent wires touch each other. Thus, in figure 1, the solid curve α can also be a trajectory in the annular space around a 'representative' single wire of a filter with filling factor $F\approx 0{\cdot}07$. The solid curve β is a much less probable event because it starts at a radius $r_{a1}>r_{aq}$. The particle, depending on local conditions, has then a higher chance of being attracted by an adjacent wire. Consequently, the theory gives only approximate guidance in the 'fuzzy' region

above r_{aq} and below $\bar{r}_a$. Beyond the value $\bar{r}_a$ the theory breaks down completely as has already been stated in §2.

In a real multiwire filter the distance between adjacent wires varies, with a certain probability distribution, over a range of values. The flow pattern is rather complicated and the capture cannot be described in simple terms. However, the volumetric flow rate through channels between wires is approximately proportional to the 4th power of the channel size, whereas the number of channels per unit cross-section of the filter is inversely proportional only to the square of their size. Consequently, the capture in larger channels is statistically more significant for the filter performance than the capture in smaller channels. This is the justification for linking the value q to the specific fluid impedance ρ_0. An exact statistical theory is beyond the scope of this paper.

3.2. Filter performance

Let N be the number of paramagnetic particles per unit volume of the fluid at the inlet of the filter. Considering unit area of the filter cross-section, the number of particles entering per unit time is $N_{\text{in}}=N\langle V_0\rangle$, where $\langle V_0\rangle$ is the average velocity of the fluid in the filter (not to be confused with $\bar{V}_0$ in (3); in general $\langle V_0\rangle \neq \bar{V}_0$). The number of particles (per unit cross-sectional area per unit time) coming out of the filter is $N_{\text{out}}=N_{\text{nc}}\langle V_e\rangle$, where N_{nc} is the number of particles per unit volume of the fluid in the filter which were not captured and $\langle V_e\rangle$ is their average escape velocity. The probability that a particle will not be captured is $(1-a^2A_a)^n$ and consequently $N_{\text{nc}}=(1-a^2A_a)^nN$. Thus, since n is large, the formula for filter performance can be written as

$$N_{\text{out}}=(\langle V_e\rangle/\langle V_0\rangle)\exp(-na^2A_a)N_{\text{in}}.$$

As all quantities in the argument of exp are known, it remains to determinate the velocity correction ratio $\langle V_e\rangle/\langle V_0\rangle$. It can be given as

$$\frac{\langle V_e\rangle}{\langle V_0\rangle}=\frac{\pi(r_{aq}^2-1)\int_{(A_a/\pi)^{1/2}}^{r_{aq}}2\pi r_a v_a\,\mathrm{d}r_a}{(\pi r_{aq}^2-A_a)\int_1^{r_{aq}}2\pi r_a v_a\,\mathrm{d}r_a} \tag{18}$$

$$=\pi\left(\frac{q}{2}-1\right)\left[-1+q+\frac{q^2}{4}\left(\ln\frac{q^2}{4}-3\right)+\left(\frac{A_a}{\pi}-1\right)^2-q\frac{A_a}{\pi}\left(\ln\frac{A_a}{\pi}-1\right)\right]$$

$$\times\left\{\left(\pi\frac{q}{2}-A_a\right)\left[-1+2q+\frac{q^2}{4}\left(\ln\frac{q^2}{4}-3\right)\right]\right\}^{-1}$$

where A_a is given by (15). It is apparent that $\langle V_e\rangle/\langle V_0\rangle$ is a quite complicated function of both q and L_a. However, this function can be approximated by its limiting value for $A_a\to\pi q/2$, i.e. by replacing $\langle V_e\rangle$ with the maximum escape velocity v_m. After performing the limiting process (or by calculating $v_m/\langle V_0\rangle$ using (2)) the expression for filter performance is obtained as

$$N_{\text{out}}=(q-2)\left[1+\frac{q}{2}\left(\ln\frac{q}{2}-1\right)\right]\left[-1+2q+\frac{q^2}{4}\left(\ln\frac{q^2}{4}-3\right)\right]^{-1}$$

$$\times\exp\left(-\frac{F}{\pi}\sum_{i=0}^{6}a_i(L_a)^{i/4}\right)N_{\text{in}} \tag{19}$$

where a_i ($i=0, 1, \ldots 6$) are functions of q, shown for $K=0{\cdot}8$ in figure 3.

The approximation of $\langle V_e\rangle/\langle V_0\rangle$ by $v_m/\langle V_0\rangle$ is quite satisfactory, since $1 \leqslant \langle V_e\rangle/\langle V_0\rangle \leqslant v_m/\langle V_0\rangle$ and $v_m/\langle V_0\rangle$ is close to unity for $q \epsilon \langle 10, 2500\rangle$, as can be found by numerical evaluation of the pre-exponential factor in (19).

The expression (19) describes the initial performance of an unloaded filter. However, it can also be used to estimate the filter performance during the filtration process, i.e. it can be applied with lower accuracy to a loaded filter. The main contributory factor to the deterioration of the filter performance, when particles are captured on the wire matrix, is the increase of the specific impedance ρ. Substituting ρ into (16) for ρ_0 and using (14), a lower value of L_a is obtained. This, when substituted in (19), accounts for the lower value of the filter performance. Other factors are disguised in changes of the coefficients a_i. They are more difficult to evaluate because the particles are captured on the sides of the wires and (2) loses its axial symmetry. For the purpose of the estimate the coefficients a_i may be considered to be approximately constant during the particle build-up process.

4. Conclusions

The mechanism of particle capture in axial filters presented in this paper is wholly consistent with the properties of real fluids. Thus the theory can be directly compared with experiment. This verification is aided by the fact that the trajectories are readily available in an analytical nearly closed form. In contrast with numerically computed solutions, if agreement with the present model is obtained in one particular instance it can be expected to be valid generally.

As a counterpart to the fluid pressure difference P_0, the magnetic pressure coefficient P_m was incorporated in the equations of motion. These equations do not depend on η, the viscosity of the fluid. Consequently, if particles are being captured on a single wire in the axial configuration, the shape of the trajectories and the capture length does not depend on η either. This conclusion can be extended to axial multiwire filters, which can be represented in the single-wire approximation. The performance of these filters is then also viscosity-independent.

The isotelic curves, defined here as the locus of initial positions of particles captured at the same distance from the origin, are in general different from the isochronal curves, defined as the locus of initial positions of particles captured after the same time. In the special case of ideal flow, both types of curves are identical, since the distribution of the fluid velocity is neglected and replaced by a constant fluid velocity V_0. This may well have some effect on the particle build-up process, which for ideal flow has recently been described by Uchiyama *et al* (1977).

The isotelic curves demarcate the capture area A_a. It is this quantity and the filling factor F which are decisive for the filter performance. When calculating the filter performance, the different values of the inflow and the escape velocities were also taken into account as the velocity correction ratio. This quantity, however, affects the filter performance much less than A_a and F, since it is close to unity and appears in (19) only as a pre-exponential factor. This may explain why the ideal flow theories can be reasonably well fitted to the bulk or average measurements.

The laminar flow theory presented here describes the capture mechanism at a single wire in a way which also, to a certain extent, takes the influence of adjacent wires into consideration. This is reflected by (15), where the capture area depends through the coefficients a_i on q and also on powers of L_a other than $\frac{1}{2}$. Thus it might be expected that the theory could apply even beyond the region of the single-wire approximation.

References

Birss R R, Gerber R and Parker M R 1976 *IEEE Trans. Magn.* **MAG-12** 892–4
Clarkson C J, Kelland D and King T B 1976 *IEEE Trans. Magn.* **MAG-12** 901–3
Cowen C, Friedlaender F J and Jaluria R 1976 *IEEE Trans. Magn.* **MAG-12** 466–70
Cummings D L, Prieve D C and Powers G J 1976 *IEEE Trans. Magn.* **MAG-12** 471–3
Landau L D and Lifshitz E M 1966 *Fluid Mechanics* (Oxford: Pergamon Press)
de Latour C and Kolm H 1975 *IEEE Trans. Magn.* **MAG-11** 1570–2
Luborsky F E and Drummond B J 1975 *IEEE Trans. Magn.* **MAG-11** 1696–1700
Uchiyama S, Kondo S, Takayasu M and Eguchi I 1976 *IEEE Trans. Magn.* **MAG-12** 895–7
Uchiyama S, Kurinobu S, Kumazawa M and Takayasu M 1977 *IEEE Trans. Magn.* **MAG-13** 1490–2
Watson J H P 1973 *J. Appl. Phys.* **44** 4209–13
—— 1975 *IEEE Trans. Magn.* **MAG-11** 1597–1599
—— 1977 *Applications of and Improvements in HGMS: Filtration Soc. Conf. London* (to be published in *Filtration and Separation*, 1978)